Published in final edited form as:
Cancer Res. 2010 December 15; 70(24): 10224–10233. doi:10.1158/0008-5472.CAN-10-3057.

Tip30 Deletion in MMTV-Neu Mice Leads to Enhanced EGFR Signaling and Development of Estrogen Receptor-Positive and Progesterone Receptor-Negative Mammary Tumors

Chengliang Zhang[1,2,5], **Mikito Mori**[1,5], **Shenglan Gao**[1,3], **Aimin Li**[1,4], **Isamu Hoshino**[1], **Mark D. Aupperlee**[1], **Sandra Z. Haslam**[1], and **Hua Xiao**[1,2,6]

[1] Department of Biomedical and Integrative Physiology, Michigan State University, East Lansing, Michigan 48824

[2] Genetics Program, Michigan State University, East Lansing, Michigan 48824

[3] Department of Biochemistry and Molecular Biology, Michigan State University, East Lansing, Michigan 48824

[4] Department of Oncology, Nanfang Hospital, Southern Medical University, Guangzhou, China 510515

Abstract

Estrogen receptor-positive and progesterone receptor-negative (ER+/PR−) breast cancers account for 15–25% of all human breast cancers and display more aggressive malignant characteristics compared to ER+/PR+ cancers. However, the molecular mechanism underlying development of ER+/PR− breast cancers still remains elusive. We show here that *Tip30* deletion dramatically accelerated the onset of mammary tumors in the MMTV-Neu mouse model of breast cancer. The mammary tumors arising in *Tip30*$^{-/-}$/MMTV-Neu mice were exclusively ER+/PR−. The growth of these ER+/PR− tumors depends not only on estrogen but also on progesterone despite the absence of detectable PR. Tip30 is predominantly expressed in ER+ mammary epithelial cells (MECs) and its deletion leads to an increase in the number of phospho-ERα (p-ERα) positive cells in mammary glands and accelerated activation of Akt in MMTV-Neu mice. Moreover, we found that Tip30 regulates the EGFR pathway through controlling endocytic downregulation of EGFR protein level and signaling. Together, these findings suggest a novel mechanism in which loss of Tip30 cooperates with Neu activation to enhance the activation of Akt signaling, leading to the development of ER+/PR− mammary tumors.

Introduction

Despite considerable success in the treatment of ER+/PR+ breast cancers with therapies directed at targeting estrogen and ERα, a substantial fraction of patients with ER+/PR− tumors do not benefit significantly from these therapies (1,2). It is estimated that 15–25% of all human breast cancers are ER+/PR− with more aggressive malignant characteristics and poorer response to selective estrogen receptor modulators (SERMs) compared to ER+/PR+

[6]Corresponding to: Hua Xiao, MD., Ph.D. Associate Professor, Department of Biomedical and Integrative Physiology, College of Human Medicine, Michigan State University, 3193 Biomedical and Physical Sciences Building, East Lansing, MI 48824-3320, 517-884-5127, Fax: 517-355-5125, xiaoh@msu.edu.
[5]These authors contributed equally to this work.

Disclosure of Potential Conflicts of Interest.
No potential conflicts of interest were disclosed

breast cancers (2–4). Moreover, 25% of ER+/PR−tumors are found to have HER2/Neu overexpression; patients with this subtype of ER+/PR− breast cancer have an extremely poor response to endocrine treatment. While several lines of evidence suggest that ER+/PR− tumors can be derived from ER+/PR+ tumors by the loss of PR expression due to anti-hormone therapy, studies indicate that ER+/PR− tumors could arise de novo from other etiological factors (5). To date, the mechanisms underlying de novo and acquired ER+/PR− breast cancer remain poorly defined. Thus, elucidation of the molecular basis of ER+/PR− breast tumor development has the potential to reveal new therapeutic targets for the treatment, and even prevention of the resistance to anti-estrogen therapy in breast cancer patients.

There are several hypotheses to explain the development of ER+/PR− breast cancers. These include inhibition of PR transcription by aberrant ER cofactors or nonfunctional ER, reduced ER activity due to lower circulating estrogen levels, hypermethylation of PR promoter, or by growth factor signaling pathways (6). Of particular interest are growth factor signaling pathways, in which aberrations are common in many human cancers (7,8). Among the growth factor receptors, HER2/Neu is the most frequently altered receptor in breast cancers. While most of HER2 positive breast cancers are ER−/PR−, only a small fraction are ER+/PR+ or ER+/PR−, suggesting that HER2 may inhibit ER expression as well as PR expression (6). This hypothesis is supported by the observation that mouse models of breast cancer harboring a HER2/Neu transgene almost exclusively develop ER−/PR− mammary tumors. Additionally, when transfected with HER2 expressing vectors, ER+/PR+ breast cancer cells exhibited a significant decrease in ER and PR expression (8). Nevertheless, the mechanism by which activation of HER2/Neu leads to development of ER−/PR−, but not ER+ breast cancer remains poorly understood.

TIP30, also known as CC3, is a 30-kDa human cellular protein that was purified as a HIV-1 Tat interacting protein (9) and its expression is altered in human liver, lung and breast cancers (10–13). Our previous studies demonstrated that Tip30-deficient mice spontaneously develop tumors in several tissues and mammary preneoplastic lesions, suggesting that TIP30 acts as a tumor suppressor (10,14). Its tumor suppressor activity is probably due to multiple mechanisms. TIP30 functions as a transcription cofactor to repress expression of genes that are involved in proliferation and apoptosis (15,16) and it can induce apoptosis as an inhibitor of nuclear import (17). In particular, TIP30 can act as a repressor of ERα-mediated c-Myc transcription in mammary glands and breast cancer cells (15). Additionally, recent evidence has highlighted that TIP30 controls endocytic downregulation of the EGFR signaling pathway in primary hepatocytes and hepatocellular carcinoma cells[7].

The multiple functions of TIP30 have prompted the speculation that TIP30 loss may contribute to mammary tumorigenesis induced by activation of oncogenes. Therefore, we aimed to determine whether Tip30 deletion enhances mammary tumorigenesis in MMTV-Neu mice. We report here that *Tip30* deletion cooperates with HER2/Neu activation to promote development of ER+/PR− mammary tumors, in part, through up-regulation of the EGFR signaling pathway. The growth of these ER+/PR− tumors appeared to depend upon both estrogen and progesterone. Thus, the *Neu+/Tip30*$^{-/-}$ mouse model may help decipher the mechanisms leading to ER+/PR− mammary tumors and identify therapeutic targets for this subgroup of tumors.

[7]C. Zhang, A. Li, X. Zhang, and H. Xiao, submitted for publication.

Results

Tip30 deletion significantly accelerates mammary tumorigenesis in MMTV-Neu mice

To investigate whether *Tip30* deletion cooperates with HER2/Neu to promote mammary tumorigenesis, we generated *Tip30* knockout mice with overexpression of Neu by crossing the MMTV-Neu transgene from MMTV-Neu mice (FVB/N-Tg; (18) into $Tip30^{-/-}$ FBV mice. $Neu+/Tip30^{-/-}$ mice appeared similar to $Neu+/Tip30^{+/+}$ mice in size and reached weaning age at the expected Mendelian frequency. A cohort of $Neu+/Tip30^{-/-}$, $Neu+/Tip30^{+/-}$ and $Neu+/Tip30^{+/+}$ female mice were monitored for 75 weeks. Mammary tumors were noted to appear earlier in $Neu+/Tip30^{-/-}$ mice compared to $Neu+/Tip30^{+/+}$ mice. Kaplan-Meier survival curves (Fig. 1A) were generated based on the time of palpable tumor formation. We observed that 50% of $Neu+/Tip30^{+/+}$ mice developed mammary tumors with a relatively long median latency of 58 weeks. The relatively longer median latency and lower frequency of tumors arising in $Neu+/Tip30^{+/+}$ mice in comparison with those in MMTV-Neu mice (18) are possibly due to only one MMTV-Neu wild-type transgene allele in $Neu+/Tip30^{+/+}$ mice. By contrast, all $Neu+/Tip30^{-/-}$ mice developed tumors at a median age of 37 weeks and 87% of $Neu+/Tip30^{+/-}$ mice developed tumors at a median age of 45 weeks. Histological analysis showed that $Neu+/Tip30^{-/-}$ tumors were poorly or moderately differentiated mammary tumors with solid or glandular growth patterns, which are morphologically similar to the mammary tumors arising in MMTV-Neu mice (Fig. 1, B1 and B2). Immunohistochemical staining of paraffin-embedded tumor sections revealed that $Neu+/Tip30^{-/-}$ or $Neu+/Tip30^{+/+}$ tumor cells were mostly Keratin (K8)-positive and α-smooth muscle actin (αSMA)-negative (Fig. 1C), indicating that $Neu+/Tip30^{-/-}$ tumors are of the luminal cell type similar to MMTV-Neu tumors (19). The presence of metastasis in the lung was observed in 4 out of 10 $Neu+/Tip30^{-/-}$ mice, whereas metastasis was detected in 1 out of 10 $Neu+/Tip30^{+/+}$ mice. These results suggest that Tip30 loss accelerates the onset of mammary luminal tumors in MMTV-Neu mice and possibly increases metastasis.

Deletion of *Tip30* results in a shift from development of ER−/PR− tumors to ER+/PR− tumors in the MMTV-Neu mouse model

It is well known that MMTV-Neu transgenic mice develop mammary tumors composed almost exclusively of ER−/PR− luminal epithelial cells. Surprisingly, we found that all $Neu+/Tip30^{-/-}$ tumors (n = 8) and 50% of $Neu+/Tip30^{+/-}$ tumors (n = 6) examined showed an ER+/PR− staining pattern (Fig. 2B), whereas 89% $Neu+/Tip30^{+/+}$ tumors (n = 9) were ER−/PR− (Fig. 2C), indicating that $Neu+/Tip30^{-/-}$ mice were more likely to develop ER+/PR− mammary tumors compared to $Neu+/Tip30^{+/+}$ mice (Table 1, 100% versus 11%; P = 0.004). These results suggest that Tip30 loss combined with activation of Neu promotes development of ER+/PR− mammary tumors.

Estrogen and progesterone promote growth of $Neu+/Tip30^{-/-}$ mammary tumors

To determine whether ER+/PR− mammary tumors arising in $Neu+/Tip30^{-/-}$ were ovarian hormone-dependent, we first transplanted small pieces of freshly dissected tumors into ovary-intact (Non-OVX) and ovariectomized (OVX) nude mice and then monitored the growth of transplanted tumor tissues. Remarkably, removal of both ovaries from recipient mice drastically reduced growth and progress of transplanted tumors, suggesting that ER+/PR− mammary tumors that developed in $Neu+/Tip30^{-/-}$ mice are ovary-dependent (Fig. 3A). Next, we transplanted small pieces of freshly dissected tumors into OVX mice supplemented with placebo, estrogen, progesterone or estrogen plus progesterone pellets (Fig. 3B and supplementary Figure 1). Surprisingly, estrogen plus progesterone strongly promoted tumor growth compared to placebo (P = 0.04), while estrogen or progesterone alone only slightly increased tumor growth compared to placebo (P > 0.05). Moreover, the progesterone antagonist RU486 was able to significantly delay the growth of $Neu+/Tip30^{-/-}$

tumors (Fig. 3C). These results suggest that both estrogen and progesterone are required for promoting growth of ER+/PR− tumors arising in *Neu+/Tip30*$^{-/-}$ mice.

The effect of progesterone on the growth of ER+/PR− tumors from *Neu+/Tip30*$^{-/-}$ mice raises the question of whether these tumor cells express any PR proteins. Because previous studies have suggested that active PRs are rapidly degraded in breast cells (20), we speculated that PR was expressed and then degraded rapidly in ER+/PR− tumors. To test this hypothesis, we examined PR-A and PR-B expression in cultured tumor cells derived from ER+/PR− tumors. Indeed, PR-A, but not PR-B, was clearly detected by Western blot analysis after cells were serum-starved and treated for 6 hours with the proteasome inhibitor, MG132 (Fig. 3D), implying that PR-A is expressed but rapidly turned over in these tumors. Together, these results suggest that estrogen and progesterone play stimulating roles in the development of ER+/PR− mammary tumors in *Neu+/Tip30*$^{-/-}$ mice.

Deletion of *Tip30* leads to a progressively increased numbers of p-ERα and p-Akt positive cells in the mammary gland from MMTV-Neu mice

The preceding data imply that Tip30 may play a key role in suppressing tumorigenesis in ERα-positive (ER+) epithelial cells. To test whether the *Tip30* gene promoter is active in ER + epithelial cells and ER+/PR− tumors, we performed immunofluorescent double staining for ERα and β-galactosidase in the mammary glands and tumors derived from *Neu+/Tip30*$^{+/-}$ mice harboring a knock-in β-galactosidase (β-Gal) gene at the *Tip30* gene locus under the control of *Tip30* promoter. The β-Gal protein was predominantly detected in ER+ mammary epithelial cells and tumor cells (Fig. 4A), indicating that the *Tip30* promoter is activated mainly in ER+ MECs and tumor cells. Given that ERα is activated through ligand binding and phosphorylation in response to estrogen and growth factor induced signaling and that *Tip30*$^{-/-}$ mice do not exhibit a significant increase in the number of ERα positive cells in the mammary gland at the age of 4 months (14), we therefore asked whether the proportion of p-ERα positive cells is altered in *Neu+/Tip30*$^{-/-}$ mammary glands. Immunohistochemical analysis was used to examine phosphorylation of ERα at Ser-171 (equivalent to Ser167 in human) in mammary glands and tumors from *Neu+/Tip30*$^{-/-}$ and *Neu+/Tip30*$^{+/+}$ mice (Fig. 4B). No significant difference in the numbers of pERα positive cells was detected between 2-month-old mammary glands from *Neu+/Tip30*$^{-/-}$ and *Neu+/Tip30*$^{+/+}$ mice (Fig. 4C). Strikingly, 12-month-old *Neu+/Tip30*$^{-/-}$ mammary glands and tumors displayed an increase in the number of p-ERα positive cells compared to *Neu+/Tip30*$^{+/+}$ mammary glands and tumors ($P < 0.05$). These results suggest that *Tip30* deletion preferentially increases the number of p-ERα positive luminal cells in the mammary gland of MMTV-Neu mice.

Akt is one of the most important downstream factors in HER2/Neu and EGFR signaling pathways that can phosphorylate ERα and regulate MEC apoptosis (21,22). Previous studies have demonstrated that expression of a constitutively active form of Akt-1 accelerates HER2/Neu-mediated mammary tumor formation (23), whereas disruption of Akt-1 delays HER2/Neu-mediated mammary tumorigenesis (24–26). To examine whether the deletion of *Tip30* affects the activation of Akt (p-Akt) in preneoplastic mammary glands from MMTV-Neu mice, we performed the immunohistochemical analysis for p-Akt in preneoplastic mammary glands from *Neu+/Tip30*$^{-/-}$ and *Neu+/Tip30*$^{+/+}$ mice at the age of 2 and 12 months. MECs at the different ages exhibit negative, weak, intermediate or strong staining for p-Akt (Fig. 5; A1, A2, A3 or A4, respectively). No significant difference in p-Akt expression levels and numbers of p-Akt-positive cells ($P = 0.678$ or 0.972, respectively) was detected between *Neu+/Tip30*$^{-/-}$ and *Neu+/Tip30*$^{+/+}$ mammary glands at 2 months of age (Fig. 5B). However, at 12 months, the number of MECs having strongly positive p-Akt staining in *Neu+/Tip30*$^{-/-}$ mammary glands was significantly increased compared to that in *Neu+/Tip30*$^{+/+}$ mammary glands (Strong staining in *Neu+/Tip30*$^{-/-}$ mammary gland:

41.4%; Strong staining in *Neu+/Tip30*$^{+/+}$ mammary gland: 9.9%; $P = 0.02$; Fig. 5C). However, there was no significant difference in the levels of p-Akt between mammary tumors from *Neu+/Tip30*$^{-/-}$ and *Neu+/Tip30*$^{+/+}$ mice (Fig. 5D). These data indicate that the relatively earlier onset of enhanced Akt activation in the mammary glands due to *Tip30* loss may contribute to accelerated mammary tumorigenesis in *Neu+/Tip30*$^{-/-}$ mice.

Tip30 deletion leads to delayed EGFR degradation and sustained EGFR signaling

Upon binding EGF, EGFR proteins are rapidly internalized and localized in early endosomes, where they are either sent back to the plasma membrane or sorted into late endosomes and lysosomes for destruction (27,28). Early endosomes serve as a platform for signaling receptors to activate specific downstream signaling until ligand-receptor dissociation occurs due to early endosomal acidification mediated by vacuolar (H^+)-ATPases (29,30). Recently, we have demonstrated that TIP30 regulates EGFR signaling by controlling endocytic downregulation of EGFR in primary hepatocytes and liver cancer cells. *Tip30* deletion impairs the fusion of Rab5 vesicles carrying vacuolar (H^+)-ATPases with early endosomes that contain internalized EGF and EGFR, leading to delayed EGFR degradation and sustained EGFR signaling[7]. Therefore, we questioned whether the increased phosphorylation of Akt and ERα in *Neu+/Tip30*$^{-/-}$ mammary gland are also caused by a similar mechanism. First, we measured the protein levels of EGFR in mammary tumors cells isolated from *Neu+/Tip30*$^{-/-}$ and *Neu+/Tip30*$^{+/+}$ mammary tumors in response to EGF treatment at various times after EGF internalization. We used an experimental approach that eliminates the interference from continuous ligand internalization and nascent protein synthesis to measure endocytic degradation of EGFR. The comparison revealed that endocytic degradation of EGFR was significantly delayed in *Neu+/Tip30*$^{-/-}$ mammary tumors cells compared to *Neu+/Tip30*$^{+/+}$ mammary tumors cells, indicating that *Tip30* deletion impairs endocytic degradation of EGFR (Fig. 6A and B).

To determine whether *Tip30* deletion can block EGFR trafficking from early endosomes to lysosomes for degradation, we tracked Alexa-488 conjugated EGF (Alexa^{488}-EGF) and EGFR in normal primary MECs isolated from *Tip30*$^{-/-}$ and *Tip30*$^{+/+}$ mice. The majority of internalized EGF dissociated from EGFR in wild type MECs two hours after EGF internalization. In contrast, they remained associated with EGFR in *Tip30*$^{-/-}$ MECs (EGF-EGFR colocalization in wild type primary MECs: 11%; EGF-EGFR colocalization in *Tip30*$^{-/-}$ primary MECs: 55%; $n = 20$, $P = 0.004$; Fig. 6C and 6D), indicating that *Tip30* deletion causes the trapping of EGF-EGFR complex in endosomes and sustained endosomal EGFR signaling. To rule out the possibility that *Tip30* deletion increased Neu transgene expression at the level of transcription, we used quantitative RT-PCR to examine the mRNA expression of Neu transgene in 5- to 9-week-old *Neu+/Tip30*$^{+/+}$ and *Neu+/Tip30*$^{-/-}$ mice and found no significant difference (data not shown). Together, these results suggest that Tip30 loss may prolong EGFR signaling, which cooperates with Neu activation to enhance Akt activation and to promote the formation of ER+/PR− tumors.

Discussion

This study was designed to investigate the relationship between HER2/Neu overexpression and *Tip30* deletion in mammary tumorigenesis by using genetically engineered mice containing both *Tip30* deletion and an MMTV-Neu transgene. Strikingly, the data demonstrate that *Tip30* deletion cooperates with Neu overexpression to promote exclusive development of ER+/PR− mammary tumors in mice. In addition, we show that Tip30 loss impairs endocytic trafficking of EGF-EGFR, delays EGFR degradation in primary MECs and tumor cells and enhances Akt and ERα phosphorylation in the mammary gland. These findings, combined with our recent observation that TIP30 formed a protein complex with ACSL4 and EndoB1 to control EGF-EGFR endocytic trafficking in hepatocytes[7], strongly

suggest a novel mechanism by which loss of Tip30 contributes to the development of ER+/PR− tumors, at least in part, through enhancing EGFR signaling in ER+ MECs.

It is not immediately obvious why *Tip30* deletion combined with Neu overexpression causes the exclusive development of ER+/PR− mammary tumors. The observation that the promoter of *Tip30* was predominantly active in ER+ MECs suggest that *Tip30* deletion may mainly affect the proliferation of ER+ cells by inducing enhanced ERα activities, thereby selecting ER+ cells to initiate tumorigenesis. Indeed, ER+/PR+ mammary tumors developed spontaneously in 22% of aged *Tip30* knockout female mice in the BALB/c genetic background[8]; and TIP30 was able to inhibit ERα-mediated transcription (15). The correlation between progressively increased p-Akt and p-ERα positive cells in *Neu+/Tip30*$^{-/-}$ mammary glands observed in this study implies that *Tip30* deletion may promote the development of ER+ mammary tumors by enhancing Akt activation and increasing active ERα positive cells. Consistent with this scenario, a previous study showed that Akt overexpression can increase the intensity of ERα staining, the number of ERα positive cells and the frequency of ER+ tumors in DMBA-treated mice (31), although it did not show whether these tumors were PR positive. Moreover, expression and phosphorylation of ERα in ER+ human breast cells is enhanced by the activation of Akt (21,31). It should be noted that enhanced Akt activation alone is insufficient for driving the tumorigenic process in mouse MECs *in vivo* (32); therefore, other mechanisms such as increased expression of c-Myc and IGF-1 induced by *Tip30* deletion may also contribute to the formation of ER+/PR− mammary tumors in MMTV-Neu mouse models (14,15).

Even thought tumors arising in *Neu+/Tip30*$^{-/-}$ mice were stained negatively for PRs and did not display significantly more PR-A/PR-B mRNA according to our quantitative RT-PCR analysis (data not shown), these ER+/PR− tumors were sensitive to progesterone stimulation and RU486 inhibition, and PR-A proteins were detectable in cultured ER+/PR− tumor cells when proteasomes were inhibited. One explanation for these observations is that PR-A is expressed in ER+/PR− tumors but rapidly turns over due to enhanced activation of EGFR and HER2/Neu *in vivo*. This explanation is supported by previous reports that PR degradation by the 26S proteasome is mediated by MAPK/ERK-induced phosphorylation at Ser294 in cultured breast cancer cells (20). It has been demonstrated that ERK1/2 activation in human cancer cells induces PR-B Ser294 phosphorylation and blocks PR-B sumoylation, which leads to two coupled events, hyperactive transcription activity and rapid turnover of PR-B proteins. PR-A was shown to be relatively resistant to these events compared to PR-B (20,33–35). In agreement with these results, we also observed significantly enhanced ERK1/2 activation at *Neu+/Tip30*$^{-/-}$ tumor periphery compared with *Neu+/Tip30*$^{+/+}$ tumor periphery (Supplementary Figure 2). Notably, we detected only PR-A after treatment with proteasome inhibitor (Figure 3D), possibly because PR-A is the dominant form in the mammary glands of mature virgin mice, whereas human breast cells express both PR-A and PR-B (36). Our observation that ER+/PR− tumors were responsive to progesterone and RU486 indicates a critical role of progesterone signaling in the growth of ER+/PR−tumors and implicates that intervention of ER+/PR− breast cancers may be achieved, in part, through suppression of PR function.

Our data seem to support the hypothesis that ER+ breast cancers arise from ER+ or otherwise estrogen-responsive progenitor cells (37). However, our data do not exclude the possibility that *Tip30* deletion may cause ER−/PR− cells to re-express ERα or promote transformed ER−/PR− luminal progenitor cells to differentiate to ER+/PR− epithelial cells. Studies on the origin of tumor cells in MMTV-Neu mice have suggested that tumor cells from this model originate from transformed luminal progenitor cells committing to ER−PR−

[8]A. Li, C. Zhang, S. Gao, R. Luo, and H. Xiao, unpublished data.

cells (38). Therefore, the cell origin of ER+/PR− tumors arising in *Neu+/Tip30*$^{-/-}$ mice remains to be determined.

Currently there remains a profound need for more effective therapies for treating HER2+/ER+/PR−breast cancers because of their poor response and development of resistance to existing therapies. Nonetheless, the majority of pre-clinical studies of ER positive breast cancer have relied on cultured cell lines or on xenograft tumor models, in which breast tumor development and progression does not accurately represent clinical human breast cancer. Alternatively, the use of genetically engineered mouse models of breast cancer has major advantages for investigating the molecular mechanism of mammary tumorigenesis, as well as developing anticancer agents. To date, there have been many mouse mammary cancer models generated by overexpression or deletion of specific genes that are associated with human breast cancer. Unfortunately, most mammary tumors arising in those animal models are ER−/PR− and do not morphologically resemble the major subtype of human breast cancer (ER+ ductal carcinoma); ER+ mammary tumors are observed in only a few genetically-engineered mouse models (39–42). To our knowledge, there has been no animal model of HER2+/ER+/PR− mammary tumors reported. Therefore, our mouse model of HER2+/ER+/PR− breast cancer provides a valuable tool for deciphering the mechanisms of HER2+/ER+/PR− breast cancer development and for testing single or combination therapies.

Materials and Methods

Mice, primary MECs and tumor cells

Tip30$^{+/-}$ mice in FBV genetic background were generated by backcrossing *Tip30*$^{+/-}$ C57BL/6 mice (14) with FBV mice seven times. *Tip30*$^{+/-}$ mice in FBV background were bred with MMTV-Neu mice (FVB/N-Tg, Jackson Laboratory) to generate *Neu+/Tip30*$^{-/-}$, *Neu+/Tip3*$^{+/-}$ and *Neu+/Tip30*$^{+/+}$ mice. Primary MECs and tumor cells were isolated and cultured as described previously (43). For tumor transplantation assays, all recipient mice were 8-week-old Nu/Nu female nude mice (Charles River). For ovariectomized mice both ovaries were removed under anesthesia. Placebo (25 mg, 90 days release), 17-estradiol (0.1 mg E2, 90-days release), Progesterone (35 mg P4, 21 days release) or E2 + P4 pellets (0.1 mg E2 + 32.5 mg P4, 90 days release) were purchased from Innovative Research of America and implanted subcutaneously in the front flanks of each mouse. RU486 was purchased from Calbiochem. Mice were sacrificed in the end of three months or when the tumor volume reached 1 cm^3. All mice were housed and cared for in the Animal Facility at Michigan State University according to institutional guidelines.

Immunofluorescence and immunohistochemistry

Immunofluorescent staining of mouse mammary tissues was performed as follow. After deparaffinization and rehydration, tissue sections were autoclaved and then incubated with primary antibody specific for ERα (MC-20, 1:50; Santa Cruz Biotechnology), p-ERα (Santa Cruz Biotechnology), PR-A (hPRa7, 1:50; Labvision), PR-B (hPRa6, 1:50; Labvision), or β-Gal (Promega) at 4 °C overnight. After PBS rinse, tissue sections were sequentially incubated for 30 min at room temperature with diluted goat anti-rabbit or mouse Alex-488 or -594-conjugated secondary antibody (1:200; Molecular Probes). Nuclei were counterstained with DAP1. Immunohistochemical staining of mouse mammary tissues was described previously (44). Immunohistochemical analysis of p-Akt at Ser-473 (1:50; Cell Signaling Technologies) and p-ERα (Santa Cruz Biotechnology) were performed as described previously (44).

EGFR internalization assay

Tip30$^{+/+}$ and *Tip30*$^{-/-}$ primary mammary epithelial cells were isolated from 2-month-old *Tip30*$^{+/+}$ and *Tip30*$^{-/-}$ female mice and cultured as previously described (14) and then serum-starved for three hours. Cells were incubated with 100 ng/ml Alexa^{488}-EGF (Invitrogen) and 20 μg/ml cycloheximide on ice for 1 hour and then washed 4 times with cold PBS before being incubated in DMEM with 20 μg/ml cycloheximide at 37 °C for two hours. Cells were fixed in 4% paraformaldehyde in PBS for 15 min, permeabilized with 0.1% Triton X-100 for 2 min and stained for EGFR. Images were obtained with a Zeiss LSM 510 Meta confocal microscope (Carl Zeiss) using Plan-Apochromat 63×/1.40 Oil objective. Pinhole size was set to 1 airy unit for all channels. All images are representative single optical sections.

Statistical Analysis

Comparisons among groups were analyzed by two-sided *t*-test or Fisher's exact test. A difference of $P < 0.05$ was considered to be statistically significant. All analyses were done with SPSS software, Version 11.5. Data are expressed as mean ± SEM.

Supplementary Material

Refer to Web version on PubMed Central for supplementary material.

Acknowledgments

We are grateful to Jill Pecha for backcrossing *Tip30* deletion allele into FBV mice and Ryan Brooks, Adam C. Edmunds, George Chen for the excellent technical assistance. We thank Ying Qin for histopathological expertise and Eran Andrechek for critical reading of the manuscript. This work was supported by grants RO1 DK066110-01 and W81XWH-08-1-0377 (to H.X.) from the NIDDK and Department of Defense and grant U01 ES/CA 012800 (to S.Z.H.) from the National Institute of Environment Health Science (NIEHS) and the National Cancer Institute (NCI), National Institutes of Health, Department of Health and Human Services. Its contents are solely the responsibility of the authors and do not necessarily represent the official views of the NIDDK, NIEHS or NCI, NIH.

References

1. Osborne CK, Schiff R, Arpino G, Lee AS, Hilsenbeck VG. Endocrine responsiveness: understanding how progesterone receptor can be used to select endocrine therapy. Breast. 2005; 14:458–65. [PubMed: 16236516]
2. Ponzone R, Montemurro F, Maggiorotto F, Robba C, Gregori D, Jacomuzzi ME, et al. Clinical outcome of adjuvant endocrine treatment according to PR and HER-2 status in early breast cancer. Ann Oncol. 2006; 17:1631–6. [PubMed: 16980602]
3. Arpino G, Weiss H, Lee AV, Schiff R, De Placido S, Osborne CK, et al. Estrogen receptor-positive, progesterone receptor-negative breast cancer: association with growth factor receptor expression and tamoxifen resistance. J Natl Cancer Inst. 2005; 97:1254–61. [PubMed: 16145046]
4. Creighton CJ, Kent Osborne C, van de Vijver MJ, Foekens JA, Klijn JG, Horlings HM, et al. Molecular profiles of progesterone receptor loss in human breast tumors. Breast Cancer Res Treat. 2009; 114:287–99. [PubMed: 18425577]
5. Kim HJ, Cui X, Hilsenbeck SG, Lee AV. Progesterone receptor loss correlates with human epidermal growth factor receptor 2 overexpression in estrogen receptor-positive breast cancer. Clin Cancer Res. 2006; 12:1013s–8s. [PubMed: 16467118]
6. Cui X, Schiff R, Arpino G, Osborne CK, Lee AV. Biology of progesterone receptor loss in breast cancer and its implications for endocrine therapy. J Clin Oncol. 2005; 23:7721–35. [PubMed: 16234531]
7. Dowsett M, Johnston S, Martin LA, Salter J, Hills M, Detre S, et al. Growth factor signalling and response to endocrine therapy: the Royal Marsden Experience. Endocr Relat Cancer. 2005; 12 (Suppl 1):S113–7. [PubMed: 16113087]

8. Konecny G, Pauletti G, Pegram M, Untch M, Dandekar S, Aguilar Z, et al. Quantitative association between HER-2/neu and steroid hormone receptors in hormone receptor-positive primary breast cancer. J Natl Cancer Inst. 2003; 95:142–53. [PubMed: 12529347]
9. Xiao H, Tao Y, Greenblatt J, Roeder RG. A cofactor, TIP30, specifically enhances HIV-1 Tat-activated transcription. Proc Natl Acad Sci U S A. 1998; 95:2146–51. [PubMed: 9482853]
10. Ito M, Jiang C, Krumm K, Zhang X, Pecha J, Zhao J, et al. TIP30 deficiency increases susceptibility to tumorigenesis. Cancer Res. 2003; 63:8763–7. [PubMed: 14695192]
11. Lee LW, Zhang DH, Lee KT, Koay ES, Hewitt RE. CC3/TIP30 expression was strongly associated with HER-2/NEU status in breast cancer. Ann Acad Med Singapore. 2004; 33:S30–2. [PubMed: 15651195]
12. Tong X, Li K, Luo Z, Lu B, Liu X, Wang T, et al. Decreased TIP30 expression promotes tumor metastasis in lung cancer. Am J Pathol. 2009; 174:1931–9. [PubMed: 19349353]
13. Zhao J, Ni H, Ma Y, Dong L, Dai J, Zhao F, et al. TIP30/CC3 expression in breast carcinoma: relation to metastasis, clinicopathologic parameters, and P53 expression. Hum Pathol. 2007; 38:293–8. [PubMed: 17097132]
14. Pecha J, Ankrapp D, Jiang C, Tang W, Hoshino I, Bruck K, et al. Deletion of Tip30 leads to rapid immortalization of murine mammary epithelial cells and ductal hyperplasia in the mammary gland. Oncogene. 2007; 26:7423–31. [PubMed: 17533366]
15. Jiang C, Ito M, Piening V, Bruck K, Roeder RG, Xiao H. TIP30 interacts with an estrogen receptor alpha-interacting coactivator CIA and regulates c-myc transcription. J Biol Chem. 2004; 279:27781–9. [PubMed: 15073177]
16. Zhao J, Lu B, Xu H, Tong X, Wu G, Zhang X, et al. Thirty-kilodalton Tat-interacting protein suppresses tumor metastasis by inhibition of osteopontin transcription in human hepatocellular carcinoma. Hepatology. 2008; 48:265–75. [PubMed: 18537194]
17. King FW, Shtivelman E. Inhibition of nuclear import by the proapoptotic protein CC3. Mol Cell Biol. 2004; 24:7091–101. [PubMed: 15282309]
18. Guy CT, Webster MA, Schaller M, Parsons TJ, Cardiff RD, Muller WJ. Expression of the neu protooncogene in the mammary epithelium of transgenic mice induces metastatic disease. Proc Natl Acad Sci U S A. 1992; 89:10578–82. [PubMed: 1359541]
19. Huang S, Li Y, Chen Y, Podsypanina K, Chamorro M, Olshen AB, et al. Changes in gene expression during the development of mammary tumors in MMTV-Wnt-1 transgenic mice. Genome Biol. 2005; 6:R84. [PubMed: 16207355]
20. Lange CA, Shen T, Horwitz KB. Phosphorylation of human progesterone receptors at serine-294 by mitogen-activated protein kinase signals their degradation by the 26S proteasome. Proc Natl Acad Sci U S A. 2000; 97:1032–7. [PubMed: 10655479]
21. Campbell RA, Bhat-Nakshatri P, Patel NM, Constantinidou D, Ali S, Nakshatri H. Phosphatidylinositol 3-kinase/AKT-mediated activation of estrogen receptor alpha: a new model for anti-estrogen resistance. J Biol Chem. 2001; 276:9817–24. [PubMed: 11139588]
22. Lannigan DA. Estrogen receptor phosphorylation. Steroids. 2003; 68:1–9. [PubMed: 12475718]
23. Hutchinson JN, Jin J, Cardiff RD, Woodgett JR, Muller WJ. Activation of Akt-1 (PKB-alpha) can accelerate ErbB-2-mediated mammary tumorigenesis but suppresses tumor invasion. Cancer Res. 2004; 64:3171–8. [PubMed: 15126356]
24. Ju X, Katiyar S, Wang C, Liu M, Jiao X, Li S, et al. Akt1 governs breast cancer progression in vivo. Proc Natl Acad Sci U S A. 2007; 104:7438–43. [PubMed: 17460049]
25. Maroulakou IG, Oemler W, Naber SP, Tsichlis PN. Akt1 ablation inhibits, whereas Akt2 ablation accelerates, the development of mammary adenocarcinomas in mouse mammary tumor virus (MMTV)-ErbB2/neu and MMTV-polyoma middle T transgenic mice. Cancer Res. 2007; 67:167–77. [PubMed: 17210696]
26. Nardulli AM, Katzenellenbogen BS. Progesterone receptor regulation in T47D human breast cancer cells: analysis by density labeling of progesterone receptor synthesis and degradation and their modulation by progestin. Endocrinology. 1988; 122:1532–40. [PubMed: 3345726]
27. Mellman I. Membranes and sorting. Curr Opin Cell Biol. 1996; 8:497–8. [PubMed: 8791461]
28. Sorkin A, Goh LK. Endocytosis and intracellular trafficking of ErbBs. Exp Cell Res. 2009; 315:683–96. [PubMed: 19278030]

29. Forgac M. Vacuolar ATPases: rotary proton pumps in physiology and pathophysiology. Nat Rev Mol Cell Biol. 2007; 8:917–29. [PubMed: 17912264]
30. Murphy JE, Padilla BE, Hasdemir B, Cottrell GS, Bunnett NW. Endosomes: a legitimate platform for the signaling train. Proc Natl Acad Sci U S A. 2009; 106:17615–22. [PubMed: 19822761]
31. Blanco-Aparicio C, Perez-Gallego L, Pequeno B, Leal JF, Renner O, Carnero A. Mice expressing myrAKT1 in the mammary gland develop carcinogen-induced ER-positive mammary tumors that mimic human breast cancer. Carcinogenesis. 2007; 28:584–94. [PubMed: 17050554]
32. Hutchinson J, Jin J, Cardiff RD, Woodgett JR, Muller WJ. Activation of Akt (protein kinase B) in mammary epithelium provides a critical cell survival signal required for tumor progression. Mol Cell Biol. 2001; 21:2203–12. [PubMed: 11238953]
33. Shen T, Horwitz KB, Lange CA. Transcriptional hyperactivity of human progesterone receptors is coupled to their ligand-dependent down-regulation by mitogen-activated protein kinase-dependent phosphorylation of serine 294. Mol Cell Biol. 2001; 21:6122–31. [PubMed: 11509655]
34. Qiu M, Lange CA. MAP kinases couple multiple functions of human progesterone receptors: degradation, transcriptional synergy, and nuclear association. J Steroid Biochem Mol Biol. 2003; 85:147–57. [PubMed: 12943699]
35. Daniel AR, Faivre EJ, Lange CA. Phosphorylation-dependent antagonism of sumoylation derepresses progesterone receptor action in breast cancer cells. Mol Endocrinol. 2007; 21:2890–906. [PubMed: 17717077]
36. Aupperlee MD, Smith KT, Kariagina A, Haslam SZ. Progesterone receptor isoforms A and B: temporal and spatial differences in expression during murine mammary gland development. Endocrinology. 2005; 146:3577–88. [PubMed: 15878961]
37. Allred DC, Brown P, Medina D. The origins of estrogen receptor alpha-positive and estrogen receptor alpha-negative human breast cancer. Breast Cancer Res. 2004; 6:240–5. [PubMed: 15535853]
38. Vaillant F, Asselin-Labat ML, Shackleton M, Forrest NC, Lindeman GJ, Visvader JE. The mammary progenitor marker CD61/beta3 integrin identifies cancer stem cells in mouse models of mammary tumorigenesis. Cancer Res. 2008; 68:7711–7. [PubMed: 18829523]
39. Liu S, Umezu-Goto M, Murph M, Lu Y, Liu W, Zhang F, et al. Expression of autotaxin and lysophosphatidic acid receptors increases mammary tumorigenesis, invasion, and metastases. Cancer Cell. 2009; 15:539–50. [PubMed: 19477432]
40. Medina D, Kittrell FS, Shepard A, Stephens LC, Jiang C, Lu J, et al. Biological and genetic properties of the p53 null preneoplastic mammary epithelium. Faseb J. 2002; 16:881–3. [PubMed: 11967232]
41. Rose-Hellekant TA, Schroeder MD, Brockman JL, Zhdankin O, Bolstad R, Chen KS, et al. Estrogen receptor-positive mammary tumorigenesis in TGFalpha transgenic mice progresses with progesterone receptor loss. Oncogene. 2007; 26:5238–46. [PubMed: 17334393]
42. Zhang X, Podsypanina K, Huang S, Mohsin SK, Chamness GC, Hatsell S, et al. Estrogen receptor positivity in mammary tumors of Wnt-1 transgenic mice is influenced by collaborating oncogenic mutations. Oncogene. 2005; 24:4220–31. [PubMed: 15824740]
43. Medina, D.; Kittrell, F. Establishment of mouse mammary cell lines. New York: Kluwer Academic/Plenum Publishers; 2000.
44. Jiang C, Pecha J, Hoshino I, Ankrapp D, Xiao H. TIP30 mutant derived from hepatocellular carcinoma specimens promotes growth of HepG2 cells through up-regulation of N-cadherin. Cancer Res. 2007; 67:3574–82. [PubMed: 17440068]
45. Ku NO, Omary MB. Keratins turn over by ubiquitination in a phosphorylation-modulated fashion. J Cell Biol. 2000; 149:547–52. [PubMed: 10791969]

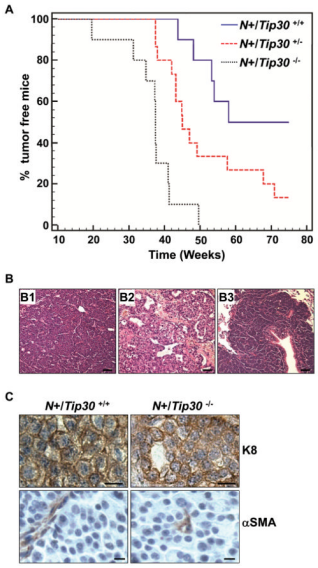

Figure 1.

Tip30 deletion significantly accelerates the onset of mammary tumors in MMTV-Neu mice. *Neu*+/*Tip30*$^{+/+}$ (n = 10), *Neu*+/*Tip30*$^{+/-}$ (n = 15) and *Neu*+/*Tip30*$^{-/-}$ (n = 10) female mice were monitored weekly for a period of 75 weeks and sacrificed at the endpoint or when tumor volume reached 0.5 cm^3. A, Kaplan-Meier analysis of survival as function of palpable tumor. The data were plotted as percentage of tumor-free animals against the time in weeks. $P \leq 0.0001$; log-rank test. B, Representative hematoxylin and eosin (H&E) stained mammary tumors arising in *Neu*+/*Tip30*$^{-/-}$ mice. A poorly differentiated adenocarcinoma with solid growth pattern (B1); A moderately differentiated adenocarcinoma with glandular growth pattern (B2); A pulmonary metastasis (B3). Scale bar, 50 μm. C, Representative immunohistochemical staining of mammary tumors for K8 (brown staining indicates presence of K8) and αSMA (lack of brown staining indicates lack of αSMA). Scale bar, 10 μm.

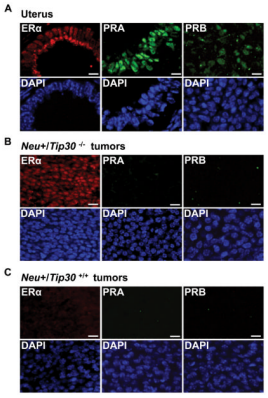

Figure 2.

Mammary tumors arising in *Neu*+/*Tip30*$^{-/-}$ mice are exclusively ER+/PR−. A-C, Representative immunofluorescent staining of ERα (red), PR-A (green) and PR-B (green) in the positive control uterus (A) and mammary tumors arising in *Neu*+/*Tip30*$^{-/-}$ mice (B) or *Neu*+/*Tip30*$^{+/+}$ mice (C). Tumor sections were stained with anti-ERα, anti-PR-A (hPRa7) or anti-PR-B (hPRa6) specific antibodies, followed by counterstaining with DAPI. Scale bar, 10 μm.

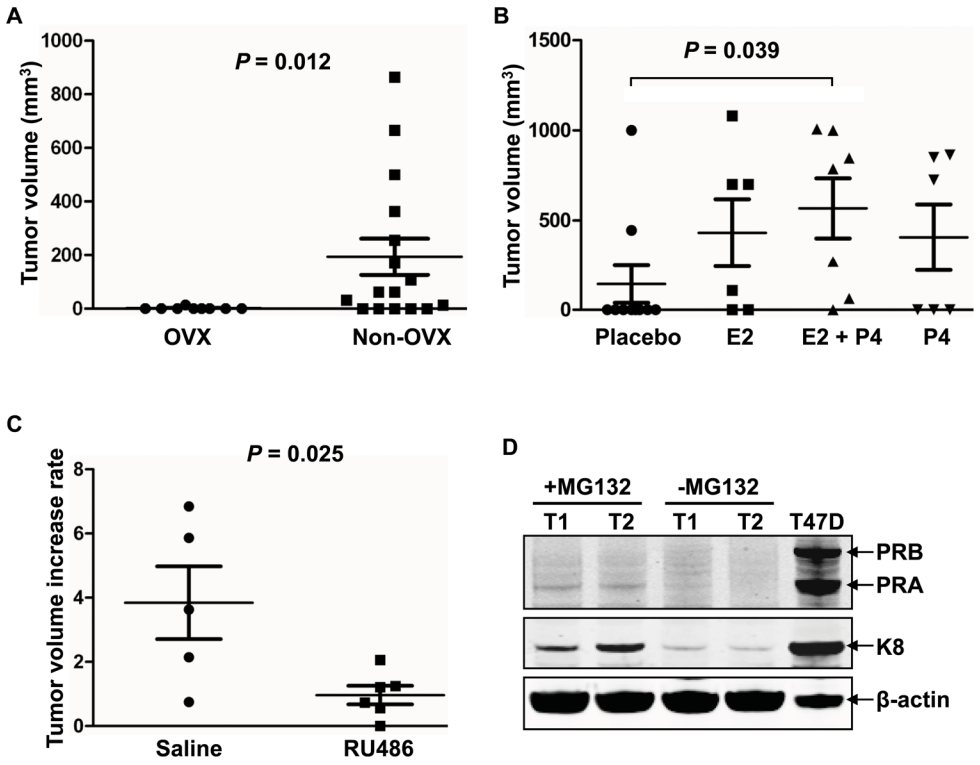

Figure 3.

Growth of ER+/PR− tumors arising in *Neu+/Tip30*$^{-/-}$ mice depends upon estrogen and progesterone. A, Two ER+/PR− mammary tumors from *Neu+/Tip30*$^{-/-}$ mice were minced and inoculated subcutaneously (s.c.) in the front flanks of ovary-intact (n = 16) or ovariectomized (n = 9) mice. The graph represents the measurements of tumors by the end of three months after transplantations or when the tumor volume reaches 1 cm^3. P = 0.012. B, Two ER+/PR− mammary tumors from *Neu+/Tip30*$^{-/-}$ mice were minced and inoculated s.c. in the front flanks of ovariectomized mice supplemented with placebo (n = 10), estrogen (E2, n = 6), progesterone (P4, n = 6) or E2 plus P4 (n = 7) pellets. The graphs show the measurements of tumor volumes by the end of three months after transplantations or when the tumor volume reaches 1 cm^3. P = 0.039 (Placebo vs E2 + P4). Note that tumor growth in two mice of the placebo group was independent of ovarian hormones. C, Growth of ER+/PR − tumors after being treated with saline/ethanol vehicle or RU486. Two ER+/PR− tumors arising in *Neu+/Tip30*$^{-/-}$ female mice were minced and inoculated s.c. to nude mice. After transplanted tumors reached approximately 0.5 cm in diameter, mice were divided into two groups to be treated with either RU486 (6.5 mg/kg body weight) or saline/ethanol vehicle solution s.c. daily for 7 days. Tumor size was measured by caliper (length and width) for another 7 days. Tumor increase rate was calculated by comparing tumor volume (1/2 × length × width^2) before and after treatment. P = 0.025. D, Primary tumor cells derived from two ER+/PR− tumors (T1 and T2) were serum-starved and cultured in the presence or absence of 10uM MG132 for 6 hours. Cell lysates were subjected to Western blot analysis with the anti-PR antibody hPRa7 that detects both PR-A and PR-B. K8 is degraded by proteasomes (45) and was blotted as a positive control for MG132 inhibition.

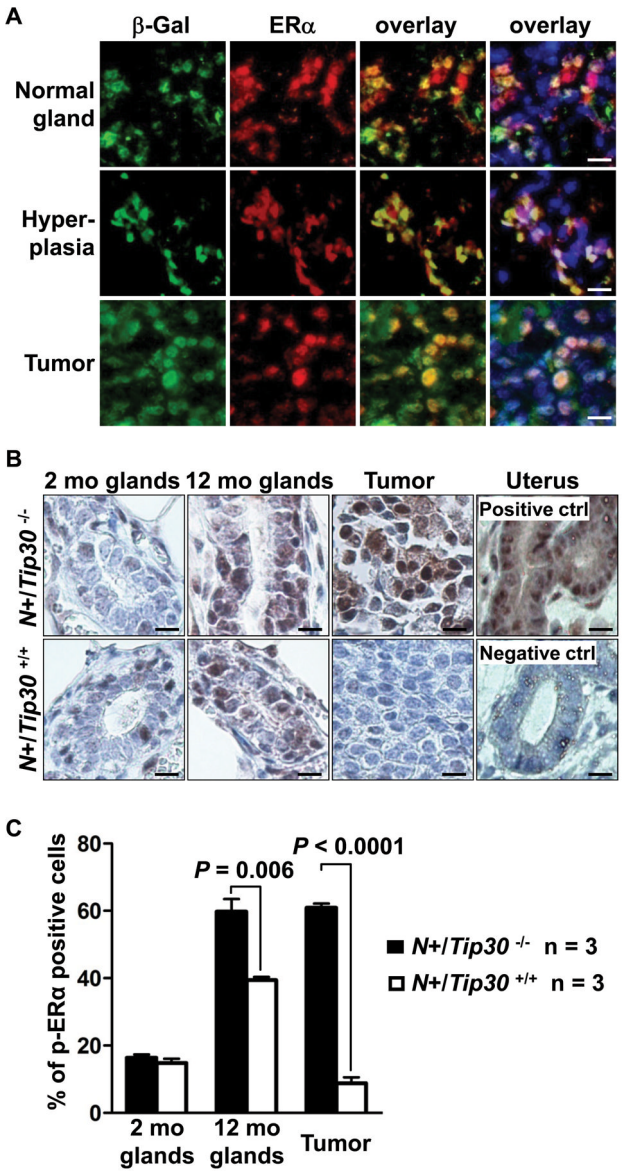

Figure 4.

Representative immunohistochemical staining of p-ERα in mammary glands and mammary tumors from *Neu+/Tip30*$^{-/-}$ and *Neu+/Tip30*$^{+/+}$ mice. A, Representative immunofluorescent double staining of mammary gland and tumor sections from a *Neu+/Tip30*$^{+/-}$ mouse for ERα (red) and β-Gal (green), followed by counterstaining with DAPI (blue). Scale bar, 10 μm. B, Representative immunohistochemical staining of p-ERα in 2-month-old and 12-month-old mammary glands and mammary tumors from *Neu+/Tip30*$^{-/-}$ and *Neu+/Tip30*$^{+/+}$ mice. As a negative control, a uterus section was stained without using the primary antibody (anti-pERα). Scale bar, 10 μm. C, Data represent means ± SEM of the percentage of p-ERα positive cells in the mammary glands and tumors derived from *Neu+/Tip30*$^{-/-}$ and *Neu+/Tip30*$^{+/+}$ mice. Positive p-ERα cells were counted in the sections of mammary glands and tumors derived from three mice of each genotype (randomly selected fields per section). 50 cells were counted per field and 10 fields were counted per mouse.

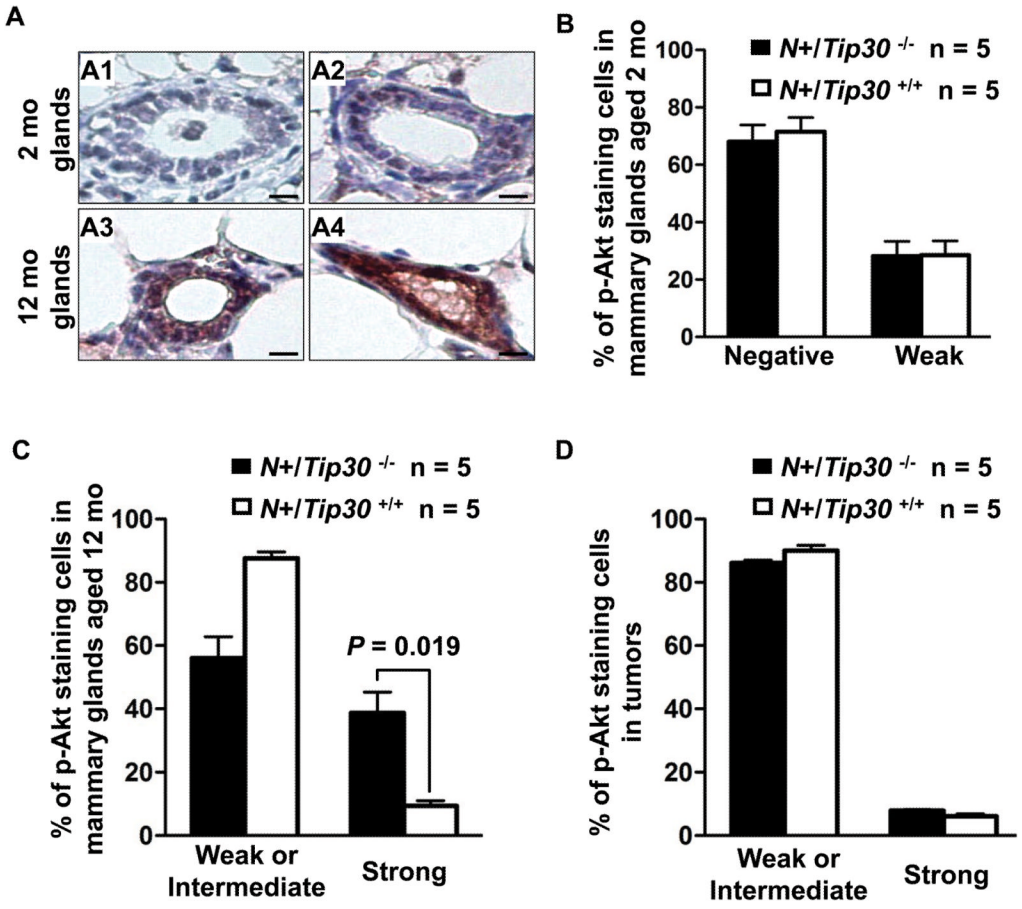

Figure 5.

Representative immunohistochemical staining for p-Akt in mammary tumors and mammary glands from *Neu*+/*Tip30*$^{-/-}$ and *Neu*+/*Tip30*$^{+/+}$ mice. A, Representative immunohistochemical staining of p-Akt in mammary glands. Staining of p-Akt in 2-month-old mammary glands ranges from negative to weak (A1 and A2) and is more intense in 12-month-old mammary glands (A3 and A4, intermediate and strong, respectively). Scale bar, 10 μm. B-D, Data represent means ± SEM of the percentage of cells that were stained positive or negative for p-Akt in 2-month-old (B) and 12-month-old (C) mammary glands and tumors (D) derived from *Neu*+/*Tip30*$^{-/-}$ and *Neu*+/*Tip30*$^{+/+}$ mice. Fifty cells were counted per field and 10 fields were counted per mouse. Data were analyzed by two-tailed *t* test.

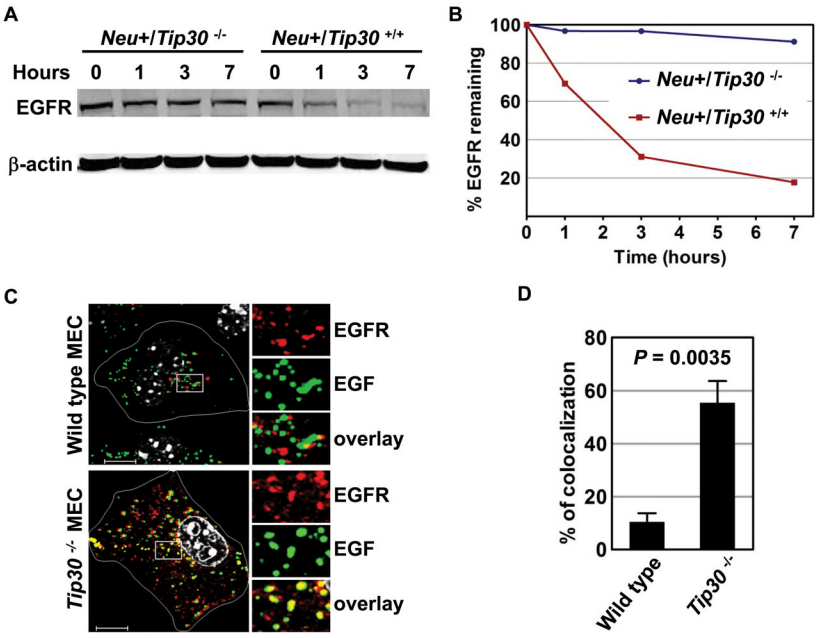

Figure 6.

Deletion of *Tip30* in MECs leads to delayed EGFR degradation. A, *Neu+/Tip30*$^{-/-}$ and *Neu+/Tip30*$^{+/+}$ mammary tumor cells were incubated with 100 ng/ml of EGF for 1 hour on ice followed by washing with cold PBS and incubating in serum-free medium containing cycloheximide (20 μg/ml) for the indicated times. Whole cell lysates were blotted with the indicated antibodies. B, Quantification of EGFR protein levels in (A) using Odyssey 2.1 software. C, primary *Tip30*$^{+/+}$ and *Tip30*$^{-/-}$ MECs were subjected to EGFR internalization analysis. Representative confocal microscopy images show the localization of EGFR (red) in endosomes after two hours of Alexa^{488}-EGF (green) internalization. Results are typical and representative of three experiments on primary cells from two mice of each genotype. Boxed areas are magnified. Representative cells are outlined in white. The colocalization of EGF and EGFR (yellow) in *Tip30*$^{-/-}$ cells is indicative of delayed endocytic degradation of EGFR; the nucleus was stained with DAPI (Grey). Scale bar, 10 μm. D, Quantitative analysis of EGF and EGFR colocalization. Twenty cells in each group were analyzed using MBF_imageJ. Pearson's colocalization coefficients were calculated and converted to percentages. $P = 0.035$.

Table 1

ERα and PR staining in mammary tumors

Tumors	ER+/PR−	ER−/PR−
Neu+/Tip30$^{-/-}$	100% (8/8)	0% (0/8)
Neu+/Tip30$^{+/-}$	50% (3/6)	50% (3/6)
Neu+/Tip30$^{+/+}$	11% (1/9)	89% (8/9)